Solar Proton Fluences for 1977–1983 Space Missions

JOSEPH H. KING*
NASA Goddard Space Flight Center, Greenbelt, Md.

The probability with which any given solar proton fluence level will be exceeded during a space mission is computed for missions to be flown during the active phase of the next solar cycle (1977–1983). This probability is a function of fluence level, proton energy threshold, and mission duration. Calculations are based on 1966–1972 data only. In estimating mission fluences, a distinction is made between ordinary and anomalously large events. Probable numbers of each type of event are estimated from Burrell's extension of Poisson statistics. Fluences of all anomalously large events are assumed to have a spectrum given by the August 1972 event, while fluences of the ordinary events are assumed to obey a log normal distribution.

I. Introduction

BECAUSE of the quasi-random nature of the occurrences, fluences, and spectra of solar proton events, solar proton mission fluences must be treated statistically. Once a space mission planner specifies a launch date, duration, and trajectory for a mission, and a risk factor (the percentage chance he is willing to take that the encountered fluence will exceed his design fluence), he selects as his design fluence the smallest fluence whose probability of being exceeded is less than or equal to the specified risk factor. The purpose of this analysis is to derive the probability of exceeding various proton fluences as a function of fluence, proton energy, and mission duration. Analyses of this nature have been generated for over ten years. They may be characterized by the data base used and the treatment of event occurrences and fluences (sampling vs various statistical techniques).

Two recent significant analyses upon which this analysis builds are those of Yucker[1] and of Burrell.[2] Yucker introduced a compound probability approach in which the probability of exceeding a mission fluence F is given as the sum over all possible numbers of events of the joint probability of the occurrence of n events and the exceeding of fluence F in those n events. He considered events from 1956–1969 and represented their fluence distribution by a single log normal function. He also estimated event occurrences by ordinary Poisson statistics. Burrell, on the other hand, used only cycle-19 data (1956–1961), but emphasized the overriding importance of very large events. He treated the event-fluence distribution in a highly idealized way (few groups of common fluence events). However, he estimated event occurrences by an extension of Poisson statistics that took into account the uncertainty in the parameter of the Poisson distribution function resulting from the small number of observations.

This analysis represents the first time data for all major cycle-20 events are presented and utilized. An extension of Yucker's compound probability approach is used in which a log normal distribution is employed to describe ordinary event fluences. However, generalizing the approach of Burrell, anomalously large events are treated separately. All such events are assumed to have a spectrum given by the August 1972 event. Finally, event occurrences are estimated separately for the two classes of events using Burrell's extension of Poisson statistics.

II. Data

Table 1 contains the basic interplanetary solar proton fluence data for solar cycle 20. The data include instantaneous peak and time-integrated fluxes, an exponential rigidity (or energy for August 1972) spectral parameter, and an indicator of whether solar protons of energies above approximately 500 Mev were observed by the Deep River Neutron Monitor. Periods that have more than one peak flux are multiflare periods. Fluxes arising from closely spaced flares have been grouped to increase the level of statistical independence in the data base.

Table 1 lists all periods of about a week for which the time-integrated flux of protons above 10 Mev exceeded $25 \times 10^7/cm^2$. This selection of 25 periods includes all (20) periods in which the >30 Mev proton flux exceeded $5.0 \times 10^6/cm^2$ and all (19) periods in which the >60 Mev flux exceeded $1.0 \times 10^6/cm^2$. The main point to note from the data of Table 1 is that the August 1972 fluxes of protons above 10, 30, 60, and 100 Mev constitute, respectively, 69%, 84%, 84%, and 83% of the fluxes (3.3×10^{10}, 9.7×10^9, 2.9×10^9, and 6.6×10^8 cm^{-2}) obtained by integrating over the entire solar cycle.

The data of Table 1 result from a variety of sources mainly associated with the IMP series of spacecraft having geocentric, highly elliptical orbits. The first three periods identified occur before the launch of IMP 4 (May 24, 1967) and are not covered as well as later periods. For all periods after the launch of IMP 4, proton flux data of Bostrom,† Lanzerotti,‡ McDonald,§ and Simpson¶ were available to the author for varying periods, either directly from the experimenter or as part of the data base of the National Space Science Data Center. All four data sets, spanning the energy range 10–100 Mev, were available for the IMP-4 period (May 1967–May 1969). A detailed study of the mutual consistency of these data revealed agreement in event-integrated fluxes typically to better then 25%.[3] As such, the data for the IMP-4 period may be considered quite reliable; and given that the IMP-5 experiments were essentially the same as those flown on IMP 4, the data for the IMP-5 period (June 1969–December 1972) may be considered similarly reliable.

The peak fluxes of Table 1 were taken directly from Bostrom's data, while the event-integrated fluxes and spectral parameters were obtained by fitting all the available spacecraft data. There is one important exception to this. An intensity-time profile is available for the flux of solar protons above 200 Mev as measured by USSR stratospheric balloon experiments during the large August 1972 events.[4] The area under the published curve has been integrated by the author to obtain an event fluence of 1.3×10^7 cm^{-2}. The error introduced by the integration technique is probably less than a factor of 2. Intrinsic errors for the data points are not discussed in Ref. 4. The >10, 30, and 60 Mev August 1972 fluences of Table 1 and the >200 Mev fluence of Ref. 4 are much better fit by an exponential in energy representation with an e-folding energy of 26.5 Mev than by other

Received November 1, 1973; revision received February 5, 1974. The author would like to thank J. I. Vette, L. R. Davis, and R. H. Hilberg for their critical reviews of this manuscript.

Index category: Radiation Protection Systems.

* Space Data Acquisition Scientist, National Space Science Data Center.

† John Hopkins University, Applied Physics Lab.
‡ Bell Telephone Labs.
§ NASA Goddard Space Flight Center.
¶ University of Chicago.

Table 1 Proton flux and spectrum data for major solar cycle 20 events

	$J_i(>10$ Mev) cm^{-2}	$J_i(>30$ Mev) cm^{-2}	$J_i(>60$ Mev) cm^{-2}	$J_i(>100$ Mev) cm^{-2}	*Ro* *MV*	$J_{pk}(>10$ Mev) cm^{-2} sec^{-1}	$J_{pk}(>30$ Mev) cm^{-2} sec^{-1}	$J_{pk}(>60$ Mev) cm^{-2} sec^{-1}
7/07– 7/09, 1966	3.8×10^7	5.0×10^6	1.5×10^6	2.3×10^5	63^a			
9/02– 9/06, 1966	1.6×10^9	8.0×10^7	1.3×10^7	1.9×10^6	50			
1/28– 2/08, 1967	7.5×10^8	1.4×10^8	5.0×10^7	1.2×10^7	78^a			
5/24– 5/30, 1967	6.6×10^8	3.8×10^7	5.7×10^6	4.4×10^5	43	1.3×10^4	4.0×10^2	2.9×10^1
						1.4×10^3	3.4×10^2	1.2×10^2
12/03–12/06, 1967	2.8×10^7	5.8×10^6	3.1×10^6	6.4×10^5	86	3.9×10^2	1.3×10^2	4.8×10^1
6/09– 6/11, 1968	4.1×10^8	1.1×10^7	1.1×10^6	1.0×10^5	38	4.4×10^3	1.6×10^2	6.8×10^1
9/28–10/06, 1968	8.6×10^7	1.2×10^7	4.9×10^6	9.2×10^5	70	4.0×10^2	2.4×10^2	1.3×10^2
						4.5×10^2	7.9×10^1	1.4×10^1
10/31–11/03, 1968	2.6×10^8	1.5×10^7	2.5×10^6	1.7×10^5	43	1.7×10^3	1.3×10^2	1.8×10^1
						1.9×10^3	1.5×10^2	1.4×10^1
11/18–11/21, 1968	1.1×10^9	2.1×10^8	7.8×10^7	1.3×10^7	70	1.1×10^4	5.1×10^3	1.2×10^{3a}
12/04–12/09, 1968	2.8×10^8	4.0×10^7	7.0×10^6	9.6×10^5	55	1.9×10^3	3.9×10^2	6.5×10^1
2/25– 3/01, 1969	6.3×10^7	2.6×10^7	1.6×10^7	7.2×10^6	159	1.1×10^3	5.2×10^2	3.0×10^{2a}
						3.5×10^2	1.2×10^2	4.6×10^1
3/30– 4/10, 1969	4.4×10^7	1.6×10^7	1.0×10^7	4.5×10^6	136	3.3×10^2	1.6×10^2	1.1×10^{2a}
4/12– 4/16, 1969	1.5×10^9	2.0×10^8	5.7×10^7	7.0×10^6	58	1.7×10^4	1.5×10^3	2.0×10^2
11/02–11/06, 1969	8.7×10^8	2.6×10^8	1.2×10^8	3.2×10^7	93	1.6×10^4	9.2×10^3	2.5×10^3
1/31– 2/02, 1970	2.8×10^7	3.4×10^6	9.2×10^5	4.0×10^5	84	3.0×10^2	7.8×10^1	2.2×10^1
3/06– 3/09, 1970	1.0×10^8	1.3×10^6	7.8×10^4	1.8×10^3	30	1.2×10^3	1.1×10^1	...
3/29– 3/31, 1970	5.9×10^7	2.1×10^7	1.2×10^7	4.8×10^6	133	8.3×10^2	2.5×10^2	8.1×10^1
7/23– 7/25, 1970	8.1×10^7	7.2×10^5	3.6×10^4	6.0×10^2	27	2.6×10^3	1.0×10^1	...
8/14– 8/17, 1970	2.6×10^8	5.0×10^6	4.0×10^5	1.2×10^4	32	2.3×10^3	3.4×10^1	3.7×10^0
	$J_i(>10)$	$J_i(>30)$	$J_i(>60)$	$J_i(>100)$	*Ro*	$J_{pk}(>10)$	$J_{pk}(>30)$	$J_{pk}(>60)$
11/05–11/08, 1970	9.6×10^7	3.5×10^6	4.4×10^5	4.0×10^4	45	5.3×10^2	2.1×10^1	5.0×10^0
1/24– 1/29, 1971	1.5×10^9	3.4×10^8	5.9×10^7	1.1×10^7	62	1.5×10^4	5.1×10^3	1.1×10^{3a}
4/06– 4/08, 1971	2.9×10^7	2.5×10^6	3.4×10^5	3.3×10^4	46	6.4×10^2	6.3×10^1	1.4×10^1
9/01– 9/05, 1971	3.8×10^8	1.6×10^8	5.5×10^7	2.1×10^7	103	4.4×10^3	2.0×10^3	8.3×10^{2a}
5/28– 6/01, 1972	6.9×10^7	6.6×10^6	1.5×10^6	2.2×10^5	57	4.9×10^2	3.4×10^1	1.5×10^1
8/04– 8/09, 1972	2.25×10^{10}	8.1×10^9	2.45×10^9	5.5×10^8	26.5(E_0)	1.1×10^6	2.6×10^5	8.0×10^{4a}
						4.4×10^4	4.8×10^3	8.7×10^{2a}

[a] > 500 Mev proton increase observed at Deep River Neutron Monitor.

standard spectral representations (exponential in rigidity, power law in energy). Accordingly, for energy thresholds between 10 and 200 Mev for the August 1972 event

$$J(>E) = 7.9\times10^9 \exp[(30-E)/26.5] \quad (1)$$

with E in Mev and J in cm^{-2}. From this representation, the J (> 100 Mev) value given in Table 1 is obtained.

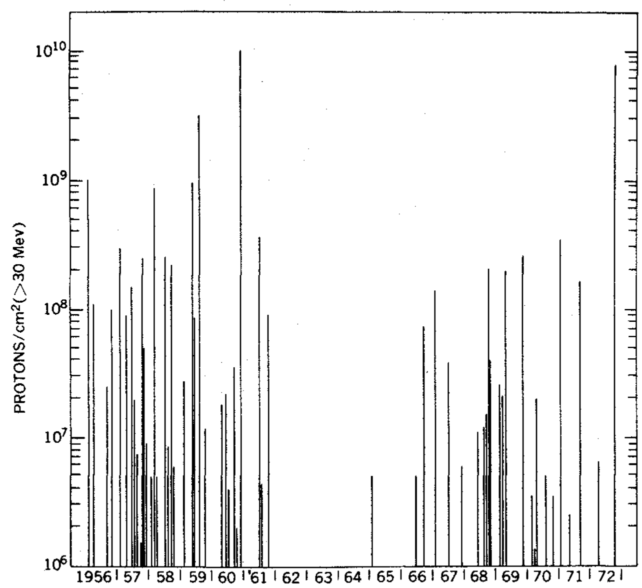

Fig. 1 Event-integrated proton fluxes above 30 Mev for the major solar events of the 19th and 20th solar cycles.

Summarizing the energy coverage of this analysis, the August 1972 integral energy spectrum to be used for missions involving the occurrence of anomalously large events is known over 10–200 Mev, while for all other missions the integral energy spectrum to be presented is reliable over 10–100 Mev.

Figure 1, containing event-integrated fluxes of solar protons of energies above 30 Mev, contrasts the solar-cycle-19 proton fluences[1] with those observed during the 20th solar cycle. The main points to be noted in Fig. 1 are 1) the lull in activity between cycles 19 and 20, 2) the generally more active character of cycle 19 in terms of event-occurrence rate and fluence amplitudes, and 3) the comparability of the August 1972 flux level with the largest cycle-19 event. Relative to the events of November 1960, which have been grouped to give the 10^{10}/cm^2 data point, estimates of the event fluence from various sources have differed by almost a factor of 10.

III. Relevance of the Data to the Future

In order to make statistical predictions about the future, two points are important. First, there should be statistical significance in the data base used; and second, the period for which the predictions are made should be similar to the period during which the data base was accumulated. From Fig. 1 it is apparent that if all the events of cycles 19 and 20 were used, a statistically more significant data base would be obtained than if only the data of one cycle or the other were used. On the other hand, the greater event-occurrence rate and the generally larger event fluences of cycle 19 demonstrate that cycles 19 and 20 were not statistically similar. From the point of view of Burrell's extension of Poisson statistics (discussed subsequently), the probability that the 19th cycle, with 32 events with $J(>30\text{ Mev}) \geqq 5\times10^6$ cm^{-2}, and any cycle with as few as 20 such events (as had the 20th)

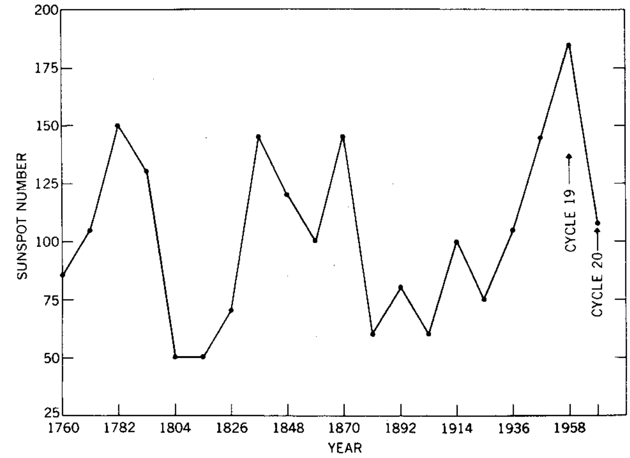

Fig. 2 Largest annual-mean sunspot numbers for past 20 solar cycles.

should have arisen from the same governing distribution is only 5%.

The relevant question becomes: What are our expectations for the statistical character of cycle 21? There is a general trend for annual-integrated solar proton fluxes to be linearly related to mean annual sunspot numbers.[5] Although this trend is not useful in predicting anomalously large fluxes such as those occurring in 1972 and as such should not be depended upon by mission planners, the largest annual mean sunspot number of a solar cycle is assumed here to be indicative of the general statistical character of that cycle's activity. Figure 2 contains a plot of such sunspot numbers for the last 20 cycles. It is quickly apparent that solar cycle 19 was very extraordinary and that cycle 20 was a very ordinary cycle. Based on the general structure of Fig. 2, it is probable that cycle 21 will be more similar to cycle 20 than to cycle 19. Other analyses suggest that cycle 21 may be characterized by sunspot numbers slightly lower than the cycle-20 numbers.[6] For this reason and because of the greater confidence one has in cycle-20 fluence values, the following analysis is restricted to the use of cycle-20 data in obtaining cycle-21 predictions.

IV. Analysis

Let F be the base-10 logarithm of a fluence (log fluence, for short) associated with all solar protons of energies greater than E encountered during a space mission of duration τ. The probability P of exceeding F in a similar mission is

$$P(>F, E; \tau) = \sum_{n=1}^{\infty} p(n, \tau; N, T) \times Q(>F, E; n) \tag{2}$$

Here $p(n, \tau; N, T)$ is the probability of occurrence of n events over duration τ, given that N events occurred during the one past observation interval of duration T. $Q(>F, E; n)$ is the probability that, given the occurrence of n events, the log of the combined fluence (again, log fluence) due to those n events will exceed F.

If $q(F, E)$ is defined as the probability density (distribution function) for the log fluence F associated with individual events, then

$$Q(>F, E; n) = \int_{-\infty}^{\infty} dx\, q(x, E) \times Q[>\log(10^F - 10^x), E; n-1] \tag{3}$$

where Q in the integrand is defined as unity if the argument of the log is zero or negative, and as zero if $x < F$ and $n = 1$ simultaneously.

Since the convolution Eq. (3) is a recursion relation in n which permits evaluation of Q for all F, E, and n, once $q(F, E)$ is specified, it is clear that the evaluation of $P(>F, E; \tau)$ is dependent on the specification of the event-occurrence probability function, $p(n, \tau; N, T)$ and the one-event log fluence distribution function, $q(F, E)$. Note that the specifications of p and of q constitute two separate problems which must be independently addressed.

The first problem encountered in the specification of $q(F, E)$ is the fact that a very large fraction (69–84%) of the cycle-20-integrated fluence occurred during one week in August 1972. It seems eminently reasonable to treat anomalously large (AL) events separately from the large number of more ordinary (OR) events, and this is done and justified in the subsequent analysis.

At some future time (after the passage of several solar cycles statistically similar to that cycle for which mission-fluence estimates are desired) there may be data available on several AL events from which a log fluence distribution function can be given, possibly with the use of extreme value statistics.[7] Alternatively, at some closer point in time, the solar physics community may have come to a sufficiently good understanding of solar flare processes that a fluence distribution may be specified theoretically. However, at this point in time there is but one AL event from a cycle (20) similar to our expectations for cycle 21. As such, no better assumption can be made than that all AL events occurring in the cycle 21 will have a spectrum identical to that observed in August 1972.

With the distinction between OR and AL events, and with the assumed commonality of spectrum of all AL events, the basic equations for the probability of exceeding log fluence F in duration τ become

$$P(>F; \tau) = \sum_{k=0}^{\infty} \sum_{n=0}^{\infty} p(k, \tau; N_{AL}, T) \times p(n, \tau; N_{OR}, T) \times Q\{>\log[10^F - (k \times 10^B)]; n\} \tag{4}$$

$$Q(>F; n) = \int_{-\infty}^{\infty} dx\, q(x) \times Q[>\log(10^F - 10^x); n-1] \tag{5}$$

Here k and n index different numbers of AL and OR events, $q(x)$ is the log fluence distribution function for OR events only, B is the log fluence for AL events, and Q in a summand or integrand is defined as unity for zero or negative values of the argument of the log. In the integrand of Eq. (5), Q is defined as zero if $x < F$ and $n = 1$ simultaneously. Note that the E dependence has been suppressed; spectral considerations will be made after the analysis is developed for a single energy.

An analytic expression for the OR event log fluence distribution function $q(F)$ must next be selected; and the parameters in the expression must be determined by the appropriate choice of data from Table 1. First of all, as in past analyses, it is assumed that F is normally distributed:

$$q(F) = [1/(2\pi)^{1/2}\sigma] \exp\{-\tfrac{1}{2}[(F - \bar{F})/\sigma]^2\} \tag{6}$$

where $\bar{F}$ is the mean log fluence and σ is the standard deviation. Such a functional dependence is very useful for analysis and represents the cycle-20 data adequately but not perfectly.

The next question to be addressed is the determination of the parameters $\bar{F}$ and σ from the data of Table 1. There are 24 OR events listed in Table 1. One may use all of these, only the larger half, or some other fraction. There is nothing more arbitrary in using the larger half rather than all the events since an arbitrary fluence threshold was initially utilized in selecting events for inclusion in Table 1. Table 2 shows the mean log fluences and corresponding standard deviations for four energy thresholds and for different selections of Table 1 events. Note that when $\bar{F}$ and

Table 2 Means and standard deviations for normal log fluence distributions

	>10 Mev	>30 Mev	>60 Mev	>100 Mev
Largest 12 ordinary (OR) events	8.81±0.29	7.92±0.45	7.41±0.44	6.78±0.47
Largest 12 OR events plus anomalously large (AL) event	8.93±0.50	8.07±0.69	7.56±0.67	6.94±0.73
All 24 OR events	8.27±0.59	7.28±0.75	6.63±0.95	5.77±1.24
All 24 OR events plus AL event	8.35±0.71	7.39±0.90	6.74±1.07	5.90±1.36
One AL event	10.35	9.91	9.39	8.74

σ are based on the 12 largest OR events, the AL-event log fluence exceeds $\bar{F}$ by more than 4σ at each energy. Note also that the relative difference between the $\bar{F}$ values determined with and without the AL event (considered as an OR event) is small everywhere and increases with increasing energy. The corresponding relative difference in σ values is much greater.

The difference in mission fluence results when selecting different $\bar{F}$ and σ from Table 2 will be examined in Sec. V. Interestingly, due to the larger standard deviation, the probability of an event fluence exceeding a sufficiently large value is greater when $\bar{F}$ and σ are determined using all 24 OR events rather than just the 12 largest OR events. For example, for a 10-Mev threshold, the probability of having an event log fluence greater than 9.3 is 4%, using either 12 or 24 OR events. But the probability for exceeding 9.8 is 0.04% or 0.5% according to whether 12 or 24 events are used. Presumably, inclusion of the next smaller 24 OR events would result in a yet greater probability for exceeding very large event fluences. This effect is clearly unrealistic, and points to the need for caution in the use of the normal log fluence distribution and the selection of the parameters. Fortunately, for the risk factors and mission durations of principal interest, log fluence probabilities are almost entirely dependent on AL-event-occurrence probability and only very weakly dependent on OR probabilities.

To complete the set of working equations required for this analysis, the probability p of observing exactly n events in a future interval of duration τ, given that N events were observed in a past interval of duration T, is given by Burrell[2] as

$$p(n,\tau;N,T)=\frac{(n+N)!}{n!N!}\times\frac{(\tau/T)^n}{[1+(\tau/T)]^{1+n+N}} \tag{7}$$

The derivation of this equation is briefly explained. Assume that the occurrence of events is random and that events, although individually rare, occur at such a rate that the number of events expected over time periods of interest is not extraordinarily large or small. The occurrences of such events is then describable by Poisson statistics

$$P(x;\mu)=\mu^x e^{-\mu}/x! \tag{8}$$

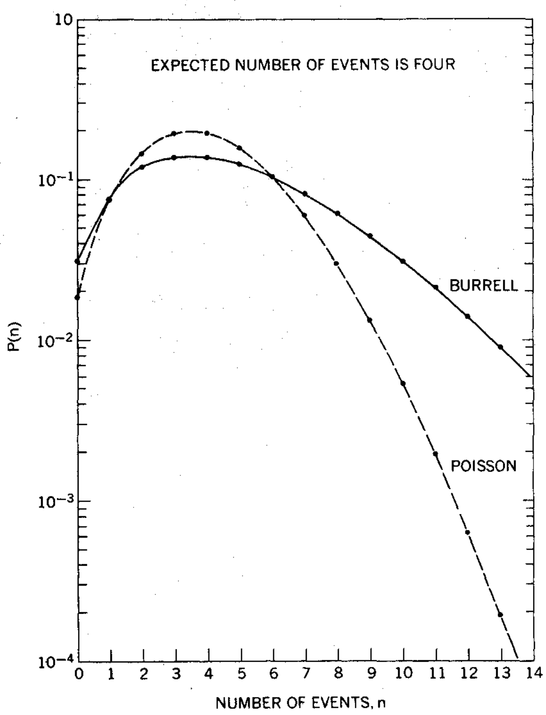

Fig. 3 Probability of observing *n* events, given that four events are expected, based on Poisson statistics and on Burrell's extension of Poisson statistics.

P is the probability of observing x events in unit time, given that the mean or expected number per unit time is μ. The parameter μ need not be an integer.

It is the point of view of statistical analyses that statistical processes are governed by noumenal distribution functions and that repeated observations yield information on the values of the parameters in any distribution function. That is, although it may

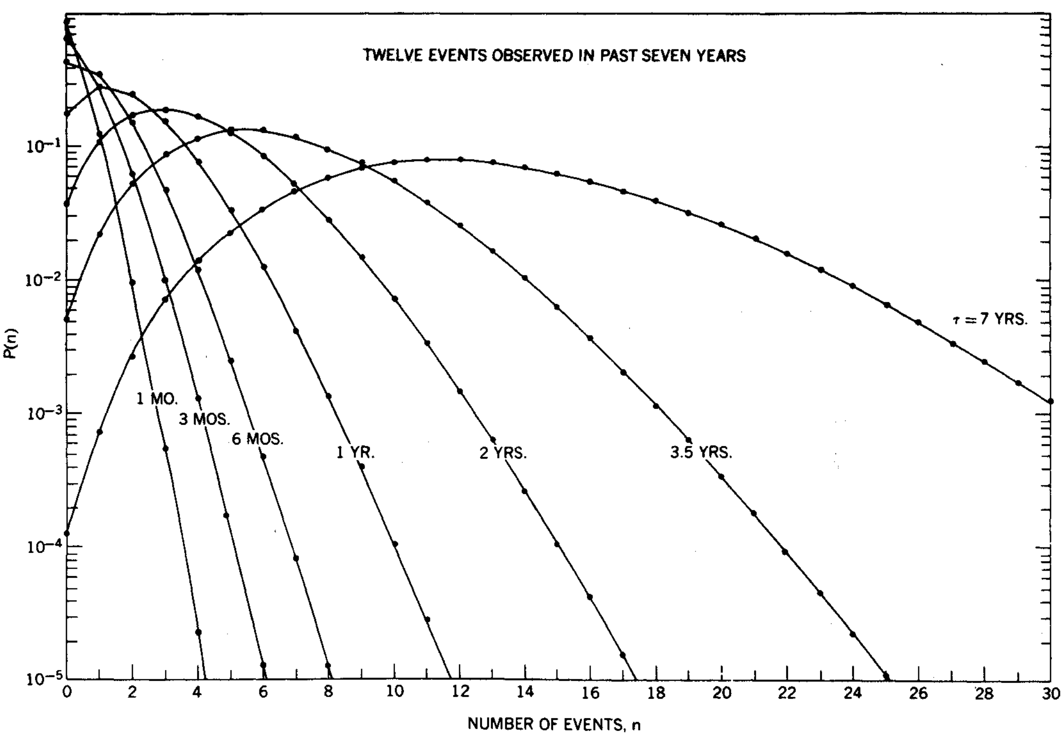

Fig. 4 Probability of observing *n* events in missions of varying durations, given the past observation of 12 events in seven years.

be asserted from the randomness of solar proton events that their occurrence should be governed by Poisson statistics, the governing Poisson distribution function may have any value of the parameter μ. A single observation of some number of events over unit time is compatible with any μ, although at differing probability levels. Several such observations help to determine which of the infinity of possible Poisson functions is in fact governing the process of interest.

In analyses prior to Burrell's which employed Poisson statistics, the mean occurrence rate (events per year or per day) as observed over one solar cycle (cycle 19) was taken as the parameter μ (i.e., as selecting which Poisson function was operative). On the other hand, Burrell took the point of view that the number of events observed over solar cycle 19 was really only one data point from which it is risky to claim which Poisson function is operative. He then reinterpreted the Poisson distribution [Eq. (8)] as giving the probability that the operative distribution is characterized by the parameter μ, given one observation of x. This is permissible in that the integral of $P(x;\mu)$ over μ from zero to infinity for any value of x is unity.

If N events were observed in past unit time, then the probability density that the operative Poisson distribution is characterized by μ is given by

$$P_1(N;\mu) = \mu^N e^{-\mu}/N! \tag{9}$$

If the operative Poisson distribution is characterized by μ, then the probability of observing n events in future unit time is

$$P_2(n;\mu) = \mu^n e^{-\mu}/n! \tag{10}$$

The probability of observing n events in future unit time, given the observation of N events in past unit time, is the probability that a given Poisson distribution is operative times that distribution's probability for n events, summed (integrated) over the infinity of possibly operative Poisson distributions. That is

$$P(n;N) = \int_0^\infty d\mu \, P_1(N;\mu) P_2(n;\mu) \tag{11}$$

Upon generalization to the case of differing past and future observation times, one obtains Eq. (7) first given by Burrell.

Quantitatively, the Burrell distribution of Eq. (7) may be compared to the simple Poisson distribution of Eq. (8) in which the parameter μ is taken directly from one past observation period. The Burrell distribution is broader than the Poisson, with greater probability of observing numbers of events far removed from the expected value and less probability near the expected value. As an example, Fig. 3 shows the situation for $\mu = N = 4$

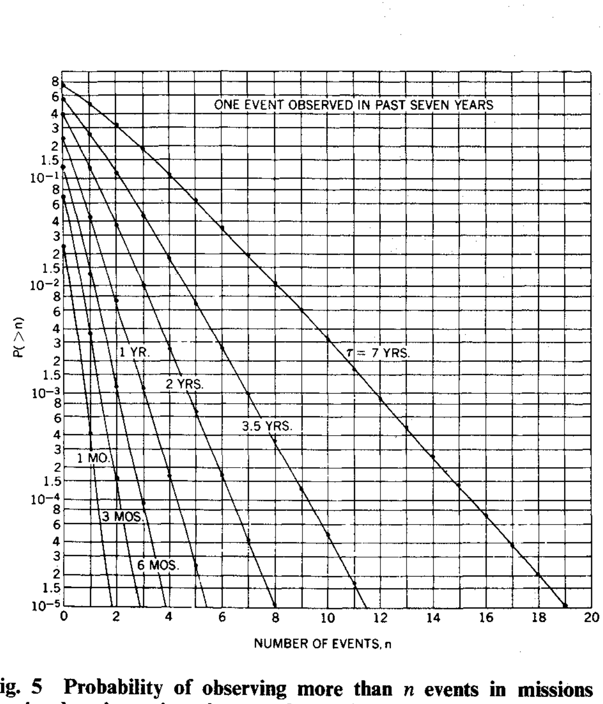

Fig. 5 Probability of observing more than n events in missions of varying durations, given the past observation of one event in seven years.

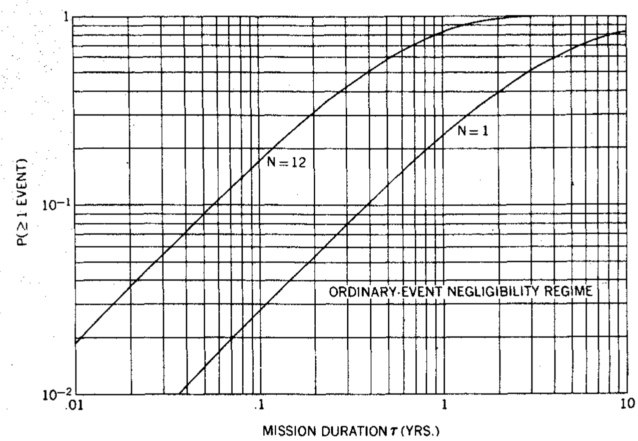

Fig. 6 Probability of observing at least one event for missions of duration τ, given the past observation of one and 12 events in seven years.

and $T = \tau = 1$. Using Stirling's formula, the ratio of Poisson to Burrell probabilities for the case $\tau = T$ and $n = KN$ ($n = K\mu$ in Poisson notation) may be written as

$$(K+1)^{1/2}\,[2/(K+1)]^{1+N(K+1)}\,e^{(K-1)N}.$$

At $n = N$, the Poisson probability is $(2)^{1/2}$ times greater than the Burrell probability for all N. At $n = 2N$, the ratio of Poisson to Burrell probabilities declines from 0.93 to 0.036 as N increases from 1 to 16, while at $n = 4N$, this ratio declines from 0.18 to 2.8×10^{-6} as N increases from 1 to 8. Thus the effect of the use of Burrell statistics instead of conventional Poisson statistics is the calculation of greater probability of exceeding a given (large) mission fluence due to the probability of encountering more events.

Figure 4 illustrates the function $p(n,\tau;N,T)$ for the case of 12 observed events (N) in the past observation period of seven years (T), for several future mission durations (τ) ranging from one month to seven years.

Figure 5 illustrates the probability of exceeding any given number of events for missions of several different durations for the case of one observed event in a past seven-year period. Figure 6 illustrates the probability of at least one event occurring during missions of varying length for the cases of one and 12 events observed in a past seven-year period.

To summarize the approach, the key equations are Eqs. (4–7). The key assumptions are: 1) the separation of ordinary and anomalously large events, 2) the commonality of spectrum for all anomalously large events, 3) the adoption of a normal distribution for the log fluences of the ordinary events, and the choice of any particular set of past events for the determination of the parameters in the distribution function, and 4) the adoption of Burrell statistics to compute probabilities of event occurrences.

V. Results

There are basically two types of results: 1) those demonstrating the extent of quantitative differences following from different assumptions, and 2) those following from what may be considered the best set of assumptions and are recommended for use.

Figure 7 is an example of the first type of result. This figure contains plots of the probability of exceeding mission log fluence F in a one-year mission for five different ways of choosing the input data. Curves V and W result from the use of ordinary (OR) and anomalously large (AL) events as described in the preceding section; the difference in the two curves results from the selection of the 12 (V) and 24 (W) largest OR log fluences in the determination of the log fluence distribution function parameters. Curve X results from the total neglect of OR events (i.e., it is assumed that the only cycle-20 activity was the one AL event of August 1972). The stepped nature of curves V, W, and X at $F > 10$ results from the discrete probabilities with which various

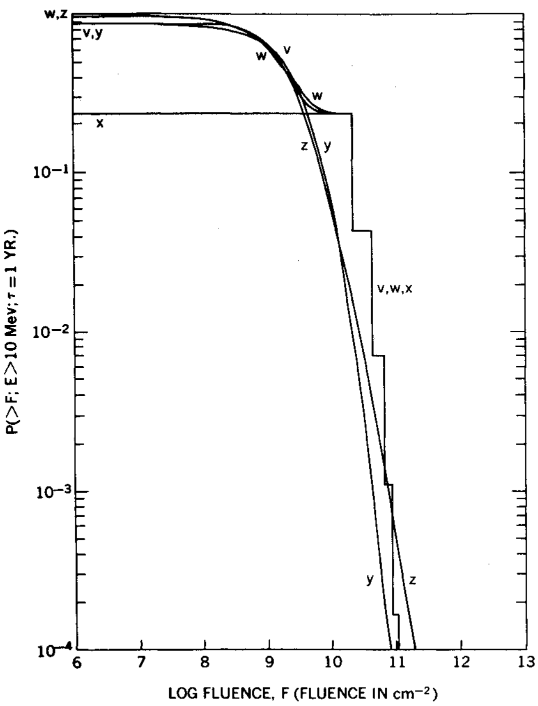

Fig. 7 Probability of exceeding log fluences F for proton energy above 10 Mev and for one-year missions, given differing ways of handling past events (see text).

numbers of AL events are exceeded. Curves Y and Z result from the failure to distinguish between OR and AL events; for these curves it was assumed that all events are OR events, describable by a log normal distribution, the parameters of which were obtained by a consideration of the largest 13 (Y) and 25 (Z) event log fluences (including August 1972). Curves Y and Z are included as a matter of interest and not as viable alternatives to the other curves since there is no justification for including in a distribution an event which contributes two to three times as much fluence as all other events combined. The input parameters for the five curves of Fig. 7 are given in the >10 Mev column of Table 2.

In comparing curves V and W, note the slight differences in structure for log fluence $F \lesssim 10$. For instance, curve V corresponds to lower probability at small log fluence because, given a smaller N_{OR} (number of past observed OR events), there is a greater chance of getting no events during the mission. The most important feature of curves V and W is that for log fluences greater than 10, these curves are indistinguishable from each other and from curve X. This indistinguishability follows from the fact that the common log fluence of the AL events is several (5.3 and 3.5 for curves V and W) σ larger than the average OR log fluence $\bar{F}$. This condition is also true at 30, 60, and 100 Mev. Thus, for all energies of interest, the following principle applies: If, for a specified mission duration, the probability of occurrence of one or more anomalously large events is greater than the acceptable risk factor, then anomalously large events dominate the mission fluence, and ordinary events are negligible. Otherwise, ordinary events are not negligible, and the full analysis must be used. A modified version of this principle was given in Ref. 2.

As an example, from Fig. 6, there is a 10% chance of getting at least one AL event during a 4.5 month mission. So to determine the fluence levels which will be exceeded with a 10% or 5% or 1% (etc.) chance, one need only consider AL events. On the other hand, to determine the (lower) fluence levels that will be exceeded with a 50% or 25% chance, one must consider OR event contributions.

Generally, the mission planner requires a design fluence for specified mission duration and risk factor Q. (Q is the percentage chance he is willing to take that the encountered fluence will exceed his design fluence.) To find a design fluence from this analysis, he first refers to Fig. 6. He locates $Q/100$ on the ordinate, and τ on the abscissa. Then if this point lies below and to the right of the $N = 1$ line, he is in the risk-factor mission-duration regime of negligibility of ordinary events. In this case, he proceeds to Fig. 5 and selects (or interpolates) the curve for his τ. He then reads off the smallest number of events whose probability of being exceeded is less than $Q/100$. Finally, he multiplies the August 1972 fluences given in Table 1 or Eq. (1) by this number of events to obtain his desired result.

As an example, suppose a mission planner is willing to take a 1% chance that his design fluence is exceeded in a one-year mission. The $[(Q/100) = 0.01, \tau = 1]$ point is in the ordinary-event-negligibility regime of Fig. 6, so he proceeds to the $\tau = 1$ year curve of Fig. 5. The smallest number of events with a probability-of-being-exceeded less than 0.01 is two. Then by doubling the August 1972 fluences of Table 1, one may be 99% confident that the mission fluence (cm^{-2}) of protons above 10, 30, 60, and 100 Mev will not exceed 4.5×10^{10}, 1.6×10^{10}, 4.9×10^{9}, and 1.1×10^{9}.

In the risk-factor mission-duration regime in which OR events are not negligible, the full analysis detailed in Sec. IV must be used. With OR event log fluence distribution function parameters based on the occurrence of 12 OR events in a past seven-year observation period (see Table 2, line 1), curves for the probability of exceeding any log fluence less than that associated with one AL event were generated for missions of various durations and for 10, 30, 60, and 100 Mev thresholds. Figure 8 shows the family of such curves for 30 Mev, after conversion from log fluence to fluence.

Comparison of the curves at other energies revealed that the representation

$$G(P, \tau, E) = G^*(P, \tau)g(E) \tag{12}$$

is very accurate, especially above 10 Mev. Here G and G^* are fluences, P the probability that the fluence will exceed G or G^*, τ the mission duration, and E the energy threshold. Figure 8 may be interpreted as giving $G^*(P, \tau)$, with the spectral function

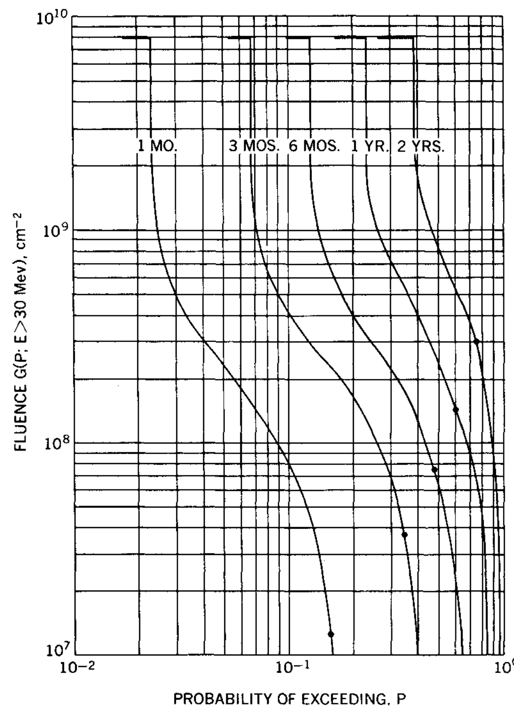

Fig. 8 Fluence of protons above 30 Mev which will be exceeded with probability P for missions of varying durations and for fluence levels less than that associated with one AL event. Heavy dots on each curve indicate galactic proton fluence to be encountered.

$g(E)$ taking the values 2.22, 1.00, 0.61, and 0.33 at 10, 30, 60, and 100 Mev, respectively. Further $g(E)$ is very well represented over the 30–100 Mev range of threshold energies as

$$g(E) = \exp[0.0158 \times (30 - E)] \qquad (13)$$

Due to the differences in standard deviations, this separation of the energy dependence introduces maximum error in fluence ($\leq 50\%$) at 10 Mev.

A set of computer runs was made to compare the results of using 12 and 24 OR events in determining parameters for short missions. For >30 Mev protons and for one-month missions, the percent differences in probabilities for exceeding any given fluence level above 10^7 cm^{-2} was not greater than 15%. For example, the probabilities of exceeding 10^8 cm^{-2} are 8.6% and 7.3%. Thus, even for missions as short as a month, the use of 12 rather than 24 input OR events does not result in significant error.

VI. Discussion

Since much of the risk-factor mission-duration plane likely to be of interest corresponds to the occurrence of at least one AL event, it is clear that the most serious deficiency of this analysis lies in the lack of understanding of AL events. Two main questions remain unanswered: 1) Does the occurrence of such events depend on the phase of the solar cycle? and 2) What are the distribution functions governing the fluence levels and spectral parameters of such events? It has been assumed in this analysis that the occurrence probability is uniform over the active phase of the solar cycle and that all such events will replicate the August 1972 event in fluence and spectral characteristics. Further, the spectral function [Eq. (1)] used for this event is greatly influenced by the >200 Mev point determined by integration of the published intensity time profile determined by USSR balloon data. At present, no better assumptions can be made. Because one has no good estimates for the range of fluences at which future anomalously large events may occur, and because the predicted mission fluence depends on the fluences of AL events, one cannot assign reliable error estimates to the results of this analysis.

With respect to the assumption of uniform probability of event occurrence, there has been a suggestion in the cycle-19 and -20 data that anomalously large events are somewhat more likely to occur early or late in the active phase of a solar cycle. This suggestion has been recently extended back to 1942 with indirect data.[8] However, in that the number of past anomalously large events is still very small, it seems unreasonable to consider the point as proven.

It is of interest to contrast the solar proton fluences derived in this analysis with galactic proton fluences. (See Ref. 9 for a recent study of galactic particle dosimetry.) The galactic proton flux, which must be regarded as a quasi-steady-state component of the interplanetary particle environment, has a value of about 1.5×10^8/cm^2-year, independent of energy in the 10–100 Mev threshold range. There is a factor of 2 variation over the solar cycle. The galactic proton data points of Fig. 8 demonstrate that for a two-year mission there is a 75% chance that solar proton fluence ($E \geq 30$ Mev) will exceed the galactic fluence, while for a one-month mission, the corresponding figure is only 16%. At higher proton energy thresholds, these percent figures will decrease. The point is that in the limits of short missions and high energies, galactic particle fluence is very important relative to solar particle fluence.

Galactic fluxes are also likely to be of prime importance for solar minimum phases. There are too few solar particle events to construct a reliable solar minimum model at this time. (See Ref. 10 for compilation of 1961–1965 events.) By 1978, after the current minimum phase, enough data may be on hand to model the mission fluences expected for the 1984–1988 period.

Note that the data used in the analysis were for interplanetary observations taken at a distance of 1 AU (Earth-sun separation distance) from the sun. As such the predictions must be used for interplanetary 1 AU missions. For spacecraft spending significant amounts of time within the geomagnetosphere, magnetic shielding will decrease the fluence expected for a given risk factor and mission duration. To obtain an estimate of this effect, Stassinopoulos and King assumed that all solar protons are excluded from the magnetosphere at geomagnetic latitudes less than 63.4° ($L < 5$ Earth radii) and that all solar protons have free access above that latitude.[11] They computed, for missions with circular orbits, the percent of the interplanetary fluence which would be encountered as a function of orbit altitude and inclination. Figure 9 is taken from their paper.

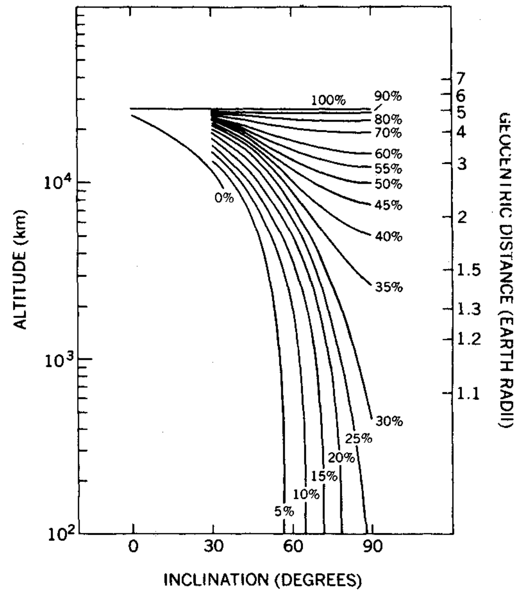

Fig. 9 Percentage of interplanetary fluence intercepted by spacecraft in circular geocentric orbits as a function of orbital altitude and inclination.

For planetary or other missions which involve much time spent significantly away from 1 AU, the heliocentric-distance dependence of event fluences must be considered.[12] Although spatial characteristics of solar-proton populations as a function of time after a flare are not well understood yet, it is clear that such fluxes are not spherically symmetric. Thus, the observation at one spatial point of an event-integrated spectrum does not permit one to say what spectrum that event would have at another spatial point. However, it seems reasonable to say that on a statistical basis, observations made at the Earth's heliolongitude would have been made at any other heliolongitude. The same may not be true of heliolatitude, although this has not yet been empirically tested. If one postulates statistical heliolatitude independence of event fluences, then a suitable helioradial dependence of event fluences is r^{-2}. This is still a rough estimate in that effects of particle deceleration in interplanetary space are neglected. Consideration of such deceleration would lead to an exponent for a given energy somewhat larger than 2. However, neglect of this effect is probably not significant in view of the assumption made regarding the anomalously large event-fluence distribution. Thus, the mission planner with a mission away from 1 AU must compute a mean helioradial distance (average of radial distances equispaced in time) for his mission, say r_m in AU, and then multiply the fluence level predicted by this analysis (for given confidence level and mission duration) by r_m^{-2}.

VII. Summary

The solar-proton-fluence data for the major solar events of the 20th solar cycle have been tabulated (see Table 1) and have been utilized in the estimation of mission fluences to be encountered in space missions of various durations flown in the 1977–1983 time period. The anomalously large event of August 1972 was considered separately from the remaining cycle-20 events. It was shown that if for a given risk factor and mission duration an AL event is expected (as indicated by Fig. 6), the ordinary events are negligible. If at least one AL event is expected, Fig. 5 is used to determine how many events are expected (see Sec. 4 for details), and the August 1972 spectrum [see Eq. (1)] is used to obtain fluences for energy thresholds up to 200 Mev. If no AL event is expected, the fluence of protons above 30 Mev which will be exceeded with probability P for mission duration τ is plotted vs P and τ in Fig. 8. For the same P and τ, the fluence of protons above any other energy between 10 and 100 Mev is obtained by multiplying the fluence of Fig. 8 by the spectral function $g(E)$ given in Sec. V.

Design fluences obtained from this analysis are directly applicable to interplanetary, 1 AU missions. Modifications for missions involving partial magnetospheric shielding and for missions away from 1 AU were discussed in Sec. VI. Solar minimum conditions and the significance of galactic particle fluences were also addressed.

References

[1] Yucker, W. B., "Solar Cosmic Ray Hazard to Interplanetary and Earth-Orbital Space Travel," *Proceedings of the 1971 National Symposium on Natural and Manmade Radiation in Space*, edited by E. A. Warman, TM X-2440, Jan. 1972, NASA, pp. 345–355.

[2] Burrell, M. O., "The Risk of Solar Proton Events to Space Missions," *Proceedings of the 1971 National Symposium on Natural and Manmade Radiation in Space*, edited by E. A. Warman, TM X-2440, Jan. 1972, NASA, pp. 310–323 (printed separately as TN D-6379, June 1971, NASA).

[3] King, J. H., "Study of Mutual Consistency of IMP 4 Solar Proton Data," NSSDC 72-14, Oct. 1972.

[4] Bazilevskaya, G. A., Stozhkov, Yu. J., Charakhchyan, A. N., and Charakhchyan, T. N., "The Energy Spectra and the Conditions of Propagation in the Interplanetary Space for Solar Protons During the Cosmic Ray Events of August 4 to 9, 1972," *Collected Papers of the 13th International Cosmic Ray Conference*, IUPAP (International Union of Pure and Applied Physics), Denver, Colo., 1973.

[5] Webber, W. R., "Sunspot Number and Solar Cosmic Ray Predictions for Cycle 20 (1965–1975) with Preliminary Estimates for Cycle 21," Rept. D2-113522-1, May 1967, The Boeing Co., Seattle, Wash.

[6] Gleissberg, W., "The Probable Behavior of Sunspot Cycle 21," *Solar Physics*, Vol. 21, No. 1, Nov. 1971, pp. 240–245.

[7] Gumbel, E. J., *Statistics of Extremes*, Columbia University Press, New York, 1954.

[8] Fritzova-Svestkova, L. and Svestka, Z., "A Comment on the Flare Activity in August 1972," *Solar Physics*, Vol. 29, No. 2, April 1973, pp. 417–419.

[9] Burrell, M. O. and Wright, J. J., "The Estimation of Galactic Cosmic Ray Penetration and Dose Rates," TN D-6600, 1972, NASA.

[10] Webber, W. R., "An Evaluation of Solar-Cosmic-Ray Events During Solar Minimum," Rept. D2-84274-1, June 1966, The Boeing Co., Seattle, Wash.

[11] Stassinopoulos, E. G. and King, J. H., "An Empirical Model of Energetic Solar Proton Fluxes with Applications to Earth Orbiting Spacecraft," *IEEE Transactions on Aerospace and Electronic Systems*, Vol. AES-10, No. 4, July 1974.

[12] Haffner, J. W., "Time Behavior of Solar Flare Particles to 5 A.U.," *Proceedings of the 1971 National Symposium on Natural and Manmade Radiation in Space*, edited by E. A. Warman, TM X-2440, Jan. 1972, NASA, pp. 336–344.